



Computer simulation of low-energy electronic excitations in atomic collision cascades

A. Duvenbeck^a, F. Sroubek^b, Z. Sroubek^c, A. Wucher^{a,*}

^a *Department of Physics, Institute of Laser and Plasma Physics, University of Duisburg-Essen, Universitätsstrasse 5, D-45117 Essen, Germany*

^b *Czech Academy of Sciences UTIA, 18208 Prague 8, Pod vodarenskou vezi 4, Czech Republic*

^c *Czech Academy of Sciences URE, 18251 Prague 8, Chaberska 57, Czech Republic*

Received 5 February 2004; received in revised form 20 April 2004

Abstract

We present a computer simulation of low-energy electronic excitations that are created in atomic collision cascades initiated by the impact of energetic particles onto a solid surface. In order to render a chemically inert system, the self-bombardment of a silver (111) surface with Ag atoms is simulated. In the model, the atomic motion following the particle impact is described by a classical molecular dynamics approach. The transfer of kinetic into electronic excitation energy is described in terms of a friction-like electronic energy loss experienced by every moving atom in the solid, thus leading to a space and time dependent density of electron–hole pair excitation energy generated in the course of the collision cascade. This energy is assumed to spread around the point of original excitation with a diffusion coefficient D and to equipartition in the Ag sp band according to a Fermi distribution characterized by an electronic temperature $T_e(\mathbf{r}, t)$. It is shown that for reasonable values of D the electronic energy deposited at the surface can be substantial, thus leading to transient electronic surface temperatures reaching several thousands of Kelvin which, for instance, can influence the ionization probabilities of sputtered atoms.

© 2004 Elsevier B.V. All rights reserved.

1. Introduction

After the impact of a fast atomic particle upon the surface of a solid, rapid movements of particles in the impact zone in the solid follow and a collision cascade is created. It is well known that the atomic motion in the solid can be analyzed in de-

tail because the interatomic forces can be modeled quite realistically and the atomic particles obey in good approximation the laws of the classical mechanics. In principle, this task can be performed in statistical terms using analytical solutions of Boltzmann transport equations [1] or by numerical computer simulations using the Monte Carlo method [2]. Alternatively, one can follow the individual trajectories of all atoms by solving the corresponding set of classical equations of motion of all atoms involved in the process. Within the laws of classical mechanics, the latter method,

* Corresponding author. Tel.: +49-201-183-4141; fax: +49-201-183-93-4141.

E-mail address: wucher@uni-essen.de (A. Wucher).

called molecular dynamics (MD), is a precise simulation of the particle motion in collision cascades and, hence, gives invaluable microscopic information on particle dynamics which cannot yet be obtained from experiments [3,4].

In practically all MD implementations that have appeared so far, the electrons in collision cascades are assumed to play only a passive role as a medium which causes a slowing down of the atomic particles [5]. This electronic energy loss is normally included in an MD calculation as a friction force proportional to the velocity of the moving atom. In the calculation of the atomic motion, any possible electronic excitation caused by this friction is generally ignored because it does not influence the atom kinetics. Moreover, at least in a metallic substrate one can expect that any excitation in the electronic system dissipates rapidly in the bulk of the solid, thus making its effective magnitude relatively small.

In some instances, however, even a weak excitation may have strong effects. When atoms are emitted (“sputtered”) from the surface as a consequence of the collision cascade, their charge and excitation state is determined either by the escaping particles’ rapid non-adiabatic passage through the surface barrier or by the electronic excitation in the solid which is transferred adiabatically to the particle. In this context, the term “surface barrier” denotes the region at and above the surface where the particle is still in an electronic interaction with the solid. In some cases, like in scattering of relatively fast projectiles that only shortly interact with the surface, the non-adiabatic processes are known to be dominant. In sputtering or multiple scattering events, however, the electronic excitation processes undergone by the substrate may play the decisive role in determining the charge and excitation states particularly of slow emitted particles.

In fact, one of the prevailing theoretical models describing the ionization probability of a sputtered atom uses the surface electron temperature T_e as a key parameter [6]. It is important to note that this temperature is assumed to describe the local state of an electron gas that – due to the short, sub-picosecond time scale on which collision cascades generally proceed – is *not* in thermal equilibrium

with the atomic motion. The magnitude of T_e , which is an extremely critical parameter of the model since it enters the ionization probability exponentially, has only been crudely estimated [7]. Moreover, the localized nature of the impact process introducing kinetic energy into the system will cause T_e to vary as a function of time and position within the surface region disturbed by a collision cascade. So far, this time and space dependence has not been accounted for. It is the purpose of the present paper to quantitatively estimate the amount of electronic excitation which is produced in such a cascade and how it distributes within the affected volume in the solid.

Unfortunately, a rigorous calculation of the electronic excitation – i.e. the ab initio solution of the Schrödinger equation of the complete system including the electronic degrees of freedom – is prohibitively complex and therefore still not practically possible. We therefore employ a number of severe semiclassical approximations in modeling the excitation processes. One of these approximations is to treat the electronic sub-system of the solid as a quasi-free electron gas, whose excitation state may be described by an electronic temperature T_e [7]. The second approximation is concerned with the process by which the kinetic energy originally imparted into the solid is coupled to and converted into electronic excitation energy. In principle, three different schemes can be used to include the excitation processes into the MD simulation of collision cascades. First, Garrison and coworkers [8–10] as well as Shapiro et al. [11,12] have invoked collisional excitation processes that are based on electron promotion in close binary encounters. This treatment has recently been utilized to describe the excitation of d-holes, thus leading to the emission of highly excited metastable atoms in sputtering [13,14]. However, the underlying physics require fairly energetic collisions which are rare in a collision cascade and lead to only few relatively large singular excitations.

Second, concepts of electron–phonon interaction have been employed to describe the energy transfer between atoms and electrons in the low-energy limit. In fact, these processes have been shown to largely dominate the energy loss experienced by the moving nuclei in the late stages of a

collision cascade, where the average kinetic energy is below 1 eV/atom and the atomic motion can be assumed to follow thermal equilibrium dynamics [15–18]. Moreover, it has been demonstrated that the description of effects like ion beam mixing or defect production ultimately requires the inclusion of electron–phonon coupling as an important cooling mechanism of the thermal spike [18]. The energy transfer can in this regime be described by a two-temperature model [16] as is also used to describe lattice heating occurring after rapid electronic excitation, for instance during electronic sputtering processes prevailing at very high projectile impact energies [19] or during laser ablation [20].

Due to the strong atomic disorder that is generally produced in an energetic collision cascade, however, the concept of phonons becomes questionable in the liquified region affected by such a cascade. Moreover, the scope of the present study is focused on relatively short time scales where collisional sputtering occurs. The relevant times are of the order of sub-ps and therefore too short to establish local thermal equilibrium. As a consequence, a two-temperature model as used to describe the thermalization of a cascade [15] cannot be applied in this time range. Moreover, average energies well above 1 eV/atom are required in the cascade to permit the sputter ejection of atoms. In this energy regime, the energy transfer between moving atoms and electrons is dominated by the electronic stopping power of individual atoms in uncorrelated motion [17]. Since the original motivation of this paper concerns the description of mechanisms leading to the excitation or ionization of sputtered particles, we employ this concept to describe the kinetic excitation of the electronic system. For the sake of simplicity, the electronic stopping power will be treated in the frame of the dielectric function theory originally formulated by Lindhard and Scharff [21]. In that way, the MD simulation naturally delivers the source term heating the electron gas as a function of location and time within the cascade volume. The temporal and spatial spread of the low-energy electronic excitations generated this way will be treated by means of a simple diffusive approach similar to that used in other work describing

electronic relaxation in collision cascades [15] or during laser ablation [22].

2. Description of the simulation

2.1. Molecular dynamics

The classical MD simulation of the atomic motion has been described in detail earlier [23]. In short, the solid is modeled by an fcc microcrystal containing 2300 atoms in nine layers. The kinetics of the system are followed by solving the classical equations of motion for all atoms, the driving forces being derived from a parametrized interaction potential that depends solely on the relative atom positions. The potential function used is the MD/MC-CEM many-body potential designed by DePristo and coworkers [24] which was fit to the bulk properties of solid silver. This potential is known to allow a reasonable description of sputtering yields, mass and energy distributions of silver particles released from a silver surface under bombardment with a number of different projectiles [25]. In order to eliminate the influence of chemical effects as much as possible, self-bombardment conditions were employed where the projectile hitting the surface is also composed of the same atoms as the solid. Since the CEM potential provides a realistic behavior at low interatomic distances, it can be directly applied to describe the interaction between the projectile and the substrate atoms as well. As mentioned above and discussed in more detail below, the energy loss experienced by a moving atom due to its interaction with the electron system of the solid is introduced into the simulation by a friction term proportional to the velocity of the atom. Open boundary conditions are used so that atoms emitted from the bottom and the sides of the crystal are allowed to take their energy with them.

The simulations described here were performed for an Ag atom with a kinetic energy of 5 keV normally incident onto an Ag(111) surface. In order to gain information about averaged quantities that can be compared to experimental data, a total of 1225 trajectories were run with different impact points, i.e. locations at the surface towards

the projectile was aimed. These impact points were uniformly distributed over the irreducible region determined by the symmetry of the (1 1 1) surface. The calculated average sputtering yield amounts to about 16 atoms/projectile, a value which is in reasonably good agreement with experimental data collected for the self-sputtering of polycrystalline silver (~ 13 atoms/projectile [26]). Moreover, the simulated mass distribution of sputtered particles (atoms and clusters) closely resembles that measured experimentally [23]. We therefore conclude that the dynamics of the collision cascade initiated by the projectile impact are described reasonably well by the simulation.

2.2. Excitation: principle

The electronic system in our model is represented by valence conduction electrons and inner shell electrons are neglected. The reason is that the inner shell electrons are not likely to be excited in low-energy cascades, particularly not at the later temporal stage, and their contribution to the charge state formation of emitted atoms is not important in the studied cases.

We thus assume that the Ag crystallite is embedded into an electron gas which is characterized by the Fermi energy ε_F and by the electron mean-free path λ . According to the prevailing theory of the electronic stopping power developed by Lindhard and Scharff [21], the energy loss per unit traveled distance of the particle moving with the kinetic energy E_k is given by

$$\frac{dE_k}{dx} = -Kv, \quad (1)$$

where v is the velocity of the particle and the coefficient K is a parameter depending upon the solid in which the particle is moving. The corresponding time derivative of E_k is given by

$$\frac{dE_k}{dt} = -Kv^2 = -AE_k, \quad (2)$$

where A is a constant equal to $(2/M)K$ and M denotes the mass of the moving particle. From (2) we obtain the expression for the time derivative of the particle velocity, which yields friction in the molecular dynamics simulation, as

$$\frac{dv}{dt} = -\frac{A}{2}v. \quad (3)$$

Probably the most appropriate theoretical description of the friction in the free electron gas of our model is due to Trubnikov and Yavlinski [27] but the Lindhard–Sharff–Schjøtt (LSS) inelastic loss model gives quantitatively similar results and is easier to handle numerically. In our paper we therefore use the LSS formula [21] for evaluating the constant A . The resulting value is $A = 2.88 \times 10^{12} \text{ s}^{-1}$ (8.75×10^{-5} a.u.) for an Ag atom moving in Ag metal.

The question remains whether the Lindhard theory, which has originally been formulated for the stopping of keV atoms in matter, is in principle applicable to the case of low-energy recoil atoms with kinetic energies in the 10 eV range as are frequently found particularly in the later stage of a collision cascade. In order to examine this point in some detail, we compare the LSS stopping cross section obtained for H in Al with recent ab initio MD calculations simulating the penetration of a low-energy H atom into the surface of an Al crystallite [28]. Comparing the total energy loss transferred into electronic excitation with the total kinetic energy as a function of time, it is found that the prediction of (2) is quantitatively fulfilled even in the kinetic energy regime of 1.5 eV and below. This finding provides a strong indication that the LSS formula can be applied without large errors even at low energies as considered here.

It should also be mentioned at this point that the (Lindhard) stopping power has been shown to significantly underestimate the energy transfer in the so-called electron phonon interaction (EPI) regime of a thermal spike at very low average kinetic energies [16,17]. As shown in [17], the friction formulae (1) and (2) are also applicable in the EPI regime with, however, modified coefficients K and A . In that sense, the electronic excitation calculated in the present paper must be regarded as a lower limit. As mentioned in the introduction, however, the present study concentrates on a relatively short time scale (< 1 ps), where the average energy is still large enough to permit collisional sputter ejection of surface particles. In this regime, we expect the electronic stopping power (ESP) to still dominate

over EPI processes (which come into play at larger times) and assume the error introduced by the neglect of EPI to be small.

The amount $dE(\mathbf{r}, t)$ of the electronic excitation energy $E(\mathbf{r}, t)$ that is transferred into the electronic system within dt by the i th particle moving with the kinetic energy $E_k^i(t)$ at the point \mathbf{r}_i and at the time t is from (2) given by $AE_k^i(t)$, and hence

$$\frac{dE(\mathbf{r}, t)}{dt} = A \sum_i E_k^i(t) \cdot \delta(\mathbf{r}_i - \mathbf{r}) = AE_k(\mathbf{r}, t). \quad (4)$$

The energy $E(\mathbf{r}, t)$, which is essentially the energy of electron–hole pairs in the metal excited by the moving particle, is rapidly carried away from the excitation spot by the motion of electron–hole pairs. This motion may be described approximately by a diffusion process characterized by a diffusion coefficient

$$D = \frac{1}{3} \lambda v_F, \quad (5)$$

where λ is the elastic mean-free path of the electrons and v_F denotes the Fermi velocity.

As discussed in [29] and also in detail below, we disregard in collision cascades the energy transfer from electrons to the lattice as a second order effect. In this case, the spatial and temporal development of $E(\mathbf{r}, t)$ is described by

$$\frac{\partial E(\mathbf{r}, t)}{\partial t} - D \nabla^2 E(\mathbf{r}, t) = \left(\frac{dE(\mathbf{r}, t)}{dt} \right)_s, \quad (6)$$

where the term on the right hand side is the source term, equal to (4) in our case.

Eq. (6) describes the development of $E(\mathbf{r}, t)$ in time and space but does not give any information how the energy is distributed between the energy levels of the solid. As the electronic energy equipartition is not known, we assume, in analogy with others [15,16,30,31], that $E(\mathbf{r}, t)$ rapidly thermalizes in the s–p conduction band at the electronic temperature T_e . This assumption can be qualitatively justified by the fact that the excitation mechanism considered here produces a large amount of low-energy excitations, the distribution of which will be relatively close to a Fermi distribution to begin with. In fact, recent ab initio simulations of H atoms penetrating into an Al metal surface reveal

transient excitation energy distributions that are close to exponential [28].

It should be noted that this situation is fundamentally different from laser excitation studies where one single, usually large energy excitation is produced per absorbed photon which then decays to ultimately form a quasi-thermal distribution of many low-energy excitations. Since relaxation times for the latter process have been measured to lie in the picosecond range [32], it is evident that thermalization of the low-energy excitation distribution produced here must proceed on a faster time scale. We therefore describe the excitation state of the electron system by a position and time dependent electron temperature T_e which is estimated from the electronic specific heat [33]

$$c_e = \frac{\pi^2}{2} \cdot n_e \cdot k_B \frac{T_e}{T_F} = C \cdot T_e \quad (7)$$

(k_B : Boltzmann constant, n_e : electron density, T_F : Fermi temperature) of the conduction electrons of the solid as

$$T_e(\mathbf{r}, t) = \sqrt{\frac{2}{C} E(\mathbf{r}, t)}. \quad (8)$$

Therefore, once $E_k(\mathbf{r}, t)$ is known from the molecular dynamics simulation, we can obtain from (6) and (8) the values of $T_e(\mathbf{r}, t)$ at any point \mathbf{r} and time t . The numerical implementation of this concept is described in the following section.

2.3. Excitation: numerical implementation

As mentioned in the previous chapter, we assume for the cascade simulation that the crystallites are embedded in a homogenous infinite electron gas. This approximation simplifies the calculation, but because the excitations can spread in all directions it also slightly underestimates the density of excitations. The proper extension to the half-space problem by inclusion of the surface is planned for a next more refined analysis. The actual numerical calculation of the excitation energy density in our case is done as follows:

The space of the crystallite is divided into small cubic elementary cells with a dimension of $2 \times 2 \times 2 \text{ \AA}^3$. The coordinates of the centers of the cells are denoted by the vectors \mathbf{r}_m where the index m

specifies the cell. For the given system there are 4000 of such cells. For each time from $t = 0$ (the impact time of the primary particle onto the surface) to $t = 750$ fs, the summed kinetic energy $E_k(\mathbf{r}_m, t)$ of atoms within each cell is calculated. For each time t_n , where t_n runs from $t = 0$ to 750 fs in intervals $\Delta t = 2.5$ fs, the values of $E_k(\mathbf{r}_m, t_n)$ are stored in the memory of the computer as a matrix. There are $750/2.5 = 300$ different times t_n and 4000 \mathbf{r}_m elements in space. We take first the matrix elements $E_k(\mathbf{r}_m, t_0)$, and according to (4) multiply them by A and Δt to obtain the excitation energy densities at (\mathbf{r}_m, t_1) . The density $AE_k(\mathbf{r}_m, t_0)$ can be treated, in this discrete representation, as a point source term in the diffusion equation (6). Already during the time interval Δt the excitation diffuses rapidly around \mathbf{r}_m and thermalizes. The solution of (6) for the point source is the Green's function that has the well known gaussian form [34]. For the first timestep, the excitation energy density $E(\mathbf{r}_k, t_1)$ at a general point \mathbf{r}_k is then given by

$$E(\mathbf{r}_k, t_1) = A \Delta t \sum_m E_k(\mathbf{r}_m, t_0) \cdot \frac{1}{(4\pi D(t_1 - t_0))^{3/2}} \cdot \exp\left(\frac{-|\mathbf{r}_m - \mathbf{r}_k|^2}{4D(t_1 - t_0)}\right), \quad (9)$$

where the sum is over all \mathbf{r}_m . Thus, according to (9), the matrix $E(\mathbf{r}_k, t_1)$ is actually the convolution of $E_k(\mathbf{r}_m, t_0)$ with the diffusion gaussian term as the convolution function.

If the diffusion coefficient D is time-independent, the values of $E(\mathbf{r}_k, t_2)$ that are due to $E_k(\mathbf{r}_m, t_0)$ can be obtained from (9) simply by substituting t_1 by t_2 , ultimately leading to the general description at arbitrary position and time

$$E(\mathbf{r}_k, t_i) = A \Delta t \sum_{n=0}^{i-1} \sum_m E_k(\mathbf{r}_m, t_n) \cdot \frac{1}{(4\pi D(t_i - t_n))^{3/2}} \cdot \exp\left(\frac{-|\mathbf{r}_m - \mathbf{r}_k|^2}{4D(t_i - t_n)}\right). \quad (10)$$

If D is allowed to vary as a function of time, a more complicated formalism must be used. For instance, if D changes from D_1 in the interval between t_1 and t_0 to D_2 in the time interval between t_2 and t_1 we must substitute, in the calculation of

$E(\mathbf{r}_k, t_2)$, the diffusion coefficient D_2 by an effective coefficient D'_2

$$D'_2 = D_2 + \frac{t_1}{t_2}(D_1 - D_2). \quad (11)$$

More generally, the constant value of D in (10) must be replaced by its average value in the time interval $t_i - t_n$. The simplicity of (11) is due to the gaussian form of the convolution function.

The final values of $E(\mathbf{r}_k, t_i)$, for any time t_i , are obtained by summing over all contributions to $E(\mathbf{r}_k, t_i)$ from $E_k(\mathbf{r}_m, t_p)$ for $t_p < t_i$. The calculation of the contributions to $E(\mathbf{r}_k, t_i)$ due to different $E_k(\mathbf{r}_m, t_p)$ follows the prescription given by (9) and (11).

3. Results and discussion

In this section, we will describe first calculations to test the application of the concepts developed above. In order to assess the magnitude of the electron temperature developing in particle impact induced collision cascades, the simulations are performed for the impact of 5-keV Ag atoms onto an unreconstructed Ag(111) surface. First, normal MD simulations are performed without the inclusion of the electronic excitation for a set of 1225 trajectories in order to obtain information about statistical quantities like the average sputtering yield as well as the influence of different impact points on the intensity of the collision cascades. Then, two particular trajectories are chosen to be treated with the much more time consuming excitation code. The first, which will in the following be referred to as no. 952, exhibits a total sputtering yield of 16 atoms/projectile that is very close to the average yield. From visualization of a number of simulations, we infer that this trajectory constitutes a normal case which is typical for the system and kinetic impact energy studied. The second, which will be called no. 207, leads to one of the highest sputtering yields (48 atoms/projectile), ejects the largest clusters and therefore represents an exceptional case where extremely large action is generated within the solid. By investigating these two cases separately, it should be possible to gain insight into the

“normal” behavior of collision cascades as well as the relatively rare events where many atoms are set in motion, thus leading to a high kinetic energy density in the cascade volume.

3.1. Diffusion coefficient

As outlined above, the central parameter of the model describing the transport of electronic excitation is the diffusion coefficient D . In the Ag conduction band the Fermi energy is calculated as 5.48 eV, corresponding to a Fermi velocity of $v_F = 1.39 \times 10^8$ cm/s. For a crystalline solid, the value of D can be estimated from (5) using the electron mean-free path λ , which under non-equilibrium conditions characterized by an electron temperature T_e and a lattice temperature T_l is given by [22,35,36]

$$\lambda = \frac{v_F}{aT_e^2 + bT_l}. \quad (12)$$

For silver, the constants in (12) are estimated as $a = 1.2 \times 10^7 \text{ K}^{-2} \text{ s}^{-1}$ and $b = 1.2 \times 10^{11} \text{ K}^{-1} \text{ s}^{-1}$ [35]. It should be noted that some controversy exists in the literature concerning the appropriate temperature dependence of λ . For instance, in their description of electron–phonon interaction in energetic displacement cascades, Flynn and Averback [18] have disregarded the role of electron–electron collisions altogether by omitting the first term in the denominator of (12). On the contrary, Koponen et al. [15,16] have argued that the influence of electron–phonon scattering should be neglected in a two-temperature model, since it is explicitly included in the electron–phonon coupling term. This would result in the omission of the second term in the denominator of (12). In the scope of the model presented here, we feel that both electron–electron and electron–phonon scattering processes should be included in the determination of the electron mean-free path, thus leading to (12). The same formula has been extensively employed in two-temperature model descriptions of laser induced excitation processes [22,36].

At room temperature ($T_e = T_l = 300 \text{ K}$), the mean-free path resulting from (12) is of the order of several tens of nanometers. Since we will later

show that lattice “temperatures” of the order of several thousands of Kelvin are rapidly reached in the collision cascade, we assume a diffusion coefficient of $D \sim 20 \text{ cm}^2/\text{s}$ for the hot but still crystalline lattice, which corresponds to value of $\lambda \sim 4.2 \text{ nm}$.

In the course of the developing collision cascade, the solid is rapidly disordered and finally completely amorphized. It is clear that the electronic energy transport properties must be altered by such a transition. In order to illustrate the time scale on which amorphization proceeds, Fig. 1 shows the pair correlation function, i.e. the distribution of interatomic distances within the simulated Ag crystallite, at various times after the projectile impact. It is apparent that the long range order is essentially lost within 300 fs, leaving only the short range order which is typical for an amorphous or liquid material. This result is practically identical for both investigated trajectories and can therefore be regarded as typical for a collision cascade.

The loss of crystallographic order will ultimately lead to a reduced value of the electron mean-free path and, hence, of the diffusion coefficient D . This phenomenon has been first discussed in [18], where it was pointed out that λ can become

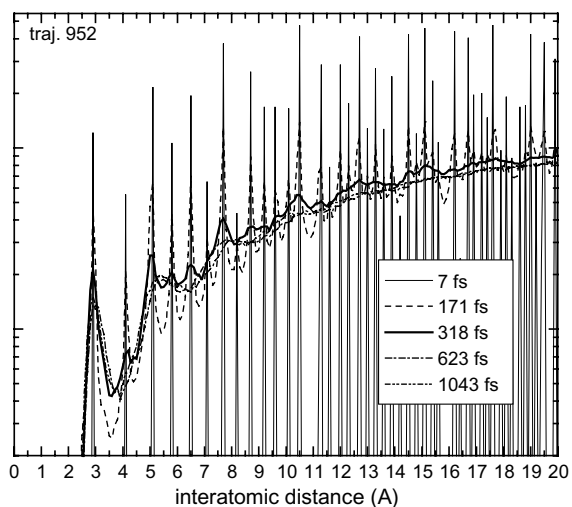


Fig. 1. Pair correlation function of interatomic distances within the investigated Ag crystallite as a function of time after the impact of a 5-keV Ag atom.

smaller than the cascade diameter and assume values of only few Å for liquid metals. In order to estimate the magnitude of the effect, we assume for the amorphized system an electron mean-free path of the order of one interatomic distance, which with (5) leads to an altered diffusion coefficient of the order of $0.5 \text{ cm}^2/\text{s}$. Therefore, the value of D will generally decrease with time as the dynamic disorder increases in the course of the time development of the collision cascade. Currently we are unable to describe this decrease quantitatively and we therefore resort to a simple approximation. In order to acknowledge the temporal variation of D , we assume a linear dependence between both limiting values within the first few hundred fs after the projectile impact and a constant value of $0.5 \text{ cm}^2/\text{s}$ at later times. The resulting electron energy densities and temperatures will be compared to those calculated under the assumption of a fixed diffusion coefficient of 20 or $0.5 \text{ cm}^2/\text{s}$, respectively.

3.2. Application on Ag

Using the formalism described above, the electronic excitation energy density has been calculated as a function of time and space for two example collision cascades referred to as trajectories 952 and 207 which lead to average and high sputter yields, respectively. In both cases, the cascade was initiated by the normal incidence of a 5-keV Ag onto an Ag(111) surface onto two different impact points. As outlined in the previous subsection, the diffusion coefficient D was chosen to decrease linearly from $20 \text{ cm}^2/\text{s}$ at $t = 0$ to $0.5 \text{ cm}^2/\text{s}$ at $t = 300 \text{ fs}$ and stay constant thereafter. The results are exemplified in Fig. 2, which shows temporal snapshots of the two-dimensional spatial distribution of (a) the total kinetic energy density and (b) the electronic excitation energy density at the surface, i.e. in the uppermost cell layer of the model. For further details, the complete simulation can be viewed electronically (<http://www.ilp.physik.uni-essen.de/wucher/>). Although the complete three-dimensional distribution is available from the simulation, the surface distributions were chosen for visualization since more than 90% of the sputtered particles originate from the topmost layer and therefore their excitation and ionization

probabilities are determined by the electron temperature at this location. Both the direct correlation between kinetic and electronic energies as described by (4) and the smearing of the electronic excitation due to diffusive transport are clearly visible.

Of note are the different scales of the energy axis on both plots in Fig. 2. In order to allow a better comparison, we average both quantities over the entire surface of our model crystallite and plot the resulting time dependence of the kinetic and electronic surface energy density in Fig. 3. It is seen that the electronic excitation energy rises quickly within the first few 10 fs, exhibits an intermediate plateau and then rises again and stays practically constant for the ps time scale on which sputtered atoms leave the surface. The second rise observed at approximately 300 fs is connected to the decrease of the energy diffusion coefficient used in the simulation. The kinetic energy density at the surface, on the other hand, shows large fluctuations in the beginning – which are due to the projectile crossing the surface cell layer – and then also levels at a fairly constant value.

Probably the most important information extracted from Fig. 3 is the fact that at all times the kinetic energy density is significantly larger than the electronic excitation energy density. This finding is important since it demonstrates that the neglect of energy flow from the electron gas to the lattice in our model is probably justified. In order to further substantiate that statement, we convert both quantities into temperatures using a lattice specific heat of $\frac{3}{2}nk_B$ and (8) for T_e . The constant C in (7) and (8) was evaluated as $C = 3.9 \times 10^{-10} \text{ eV}/\text{Å}^3 \text{ K}^2$ using the electron density $n_e = 5.85 \times 10^{22} \text{ cm}^{-3}$ and Fermi temperature $T_F = 6.4 \times 10^4 \text{ K}$ of silver ([33]). The results are plotted in Fig. 4. Note that the lattice “temperature” determined this way has no real physical meaning since the particle kinetics within the collision cascade do not necessarily follow Maxwell–Boltzmann statistics. Moreover, no correction for possible collective motion velocity components (which for a real temperature determination would have to be subtracted from the individual particle velocities in a cell [36]) has been performed. Nevertheless, it is evident that – although the specific heat of the electron gas is

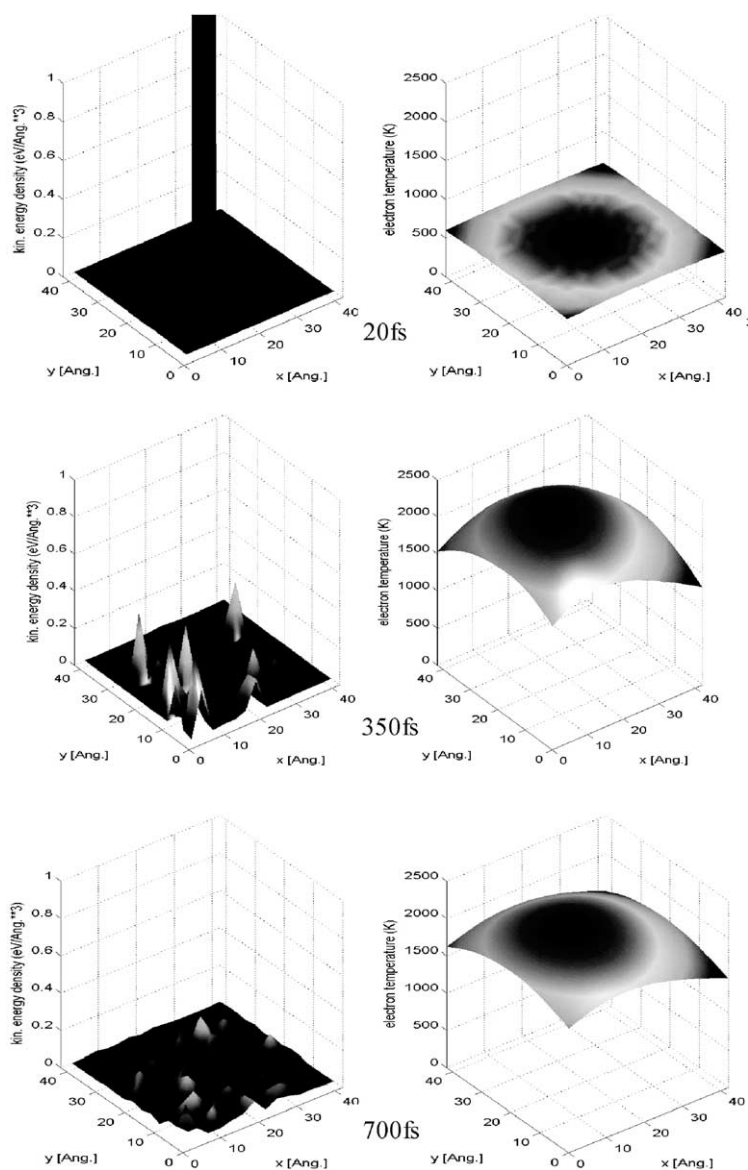


Fig. 2. Snapshots of the two-dimensional spatial distribution of (a) the total kinetic energy density and (b) the electron temperature at the surface for three different times after the projectile impact. The data were calculated for a particular collision cascade described as trajectory 207 in the text. In order to illustrate the observed variation, the gray scale code was for each individual image chosen such as to extend over the observed range between minimum and maximum values.

much lower than that of the lattice – the electron temperature never significantly exceeds the lattice “temperature”. Therefore, also a two-temperature model as used frequently to describe lattice heating by electronic excitation [30] would predict negli-

gible energy flow back from the electron system into the lattice dynamics.

It is of course essential to investigate how the particular choice of the diffusion coefficient D influences the simulated results. In order to

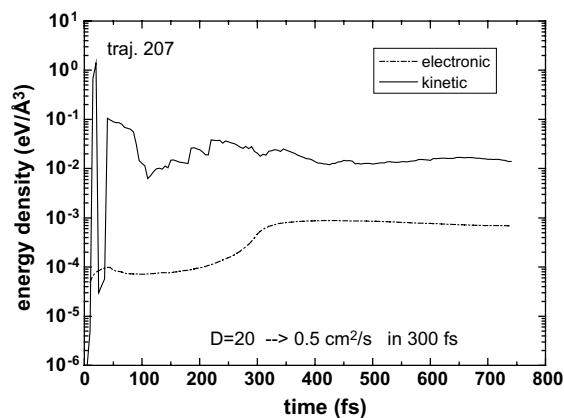


Fig. 3. Average total kinetic and electronic excitation energy density at the surface versus time after the projectile impact. The data were calculated for a particular collision cascade described as trajectory 207 in the text.

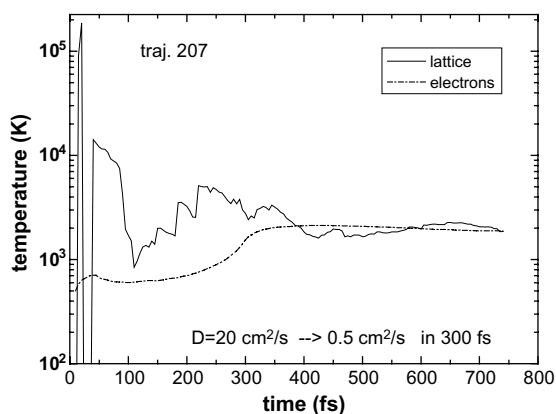


Fig. 4. Average lattice "temperature" and electron temperature at the surface versus time after the projectile impact. The data were converted from the energy densities depicted in Fig. 3.

visualize the surface distribution of the calculated electronic energy density and electron temperature, we plot radial distributions that are obtained in the following way. First, the surface electron energy density is averaged over four cells that are located in the directions parallel to the crystallite edges at a certain radial distance r from that cell containing the impact point. The resulting surface energy density calculated for a constant diffusion coefficient as a function of time after the projectile impact is depicted in Fig. 5. The data have been

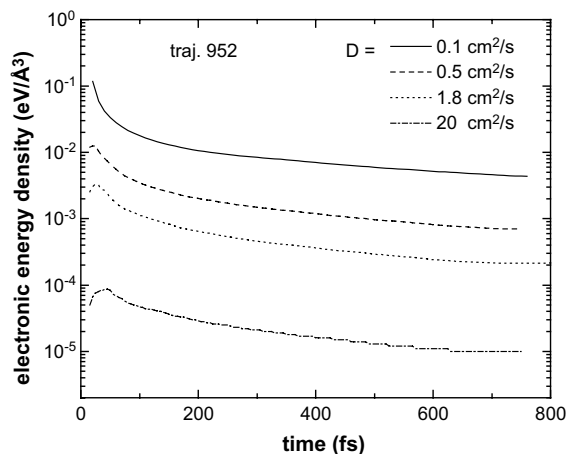


Fig. 5. Surface electronic excitation energy density at the impact point versus time after projectile impact. The data have been calculated for trajectory no. 952 (see text) using a constant electron energy diffusion coefficient as displayed.

calculated for trajectory 952, the corresponding curves for trajectory 207, however, look very similar. In order to illustrate the influence of energy transport, different values of the diffusion coefficient were used spanning the range from an unrealistically low value of $0.1 \text{ cm}^2/\text{s}$ to $D = 20 \text{ cm}^2/\text{s}$ which is assumed to be appropriate for the crystalline solid. It is seen that the magnitude of the electronic excitation roughly scales with the inverse of D . Moreover, the surface energy density rapidly goes through a maximum at very short times below 50 fs which is produced by the large energy loss of the projectile crossing the surface layer and then decays again. Note that although the figure seems to suggest that a "steady state" is reached after about 1 ps, it is clear that in the limit of large time the electronic interaction must dissipate in the bulk of the solid and, hence, the excitation energy density must go to 0.

Second, the average energy density is converted into surface electron temperature by means of (8). Again, the results are plotted as a function of time after the projectile impact for different values of r . Fig. 6 shows such a plot calculated for trajectories 207 and 952 for the case of a constant diffusion coefficient of $D = 20$ and $0.5 \text{ cm}^2/\text{s}$, respectively. As outlined in Section 3.1, these values are assumed to correspond to an ordered and to a

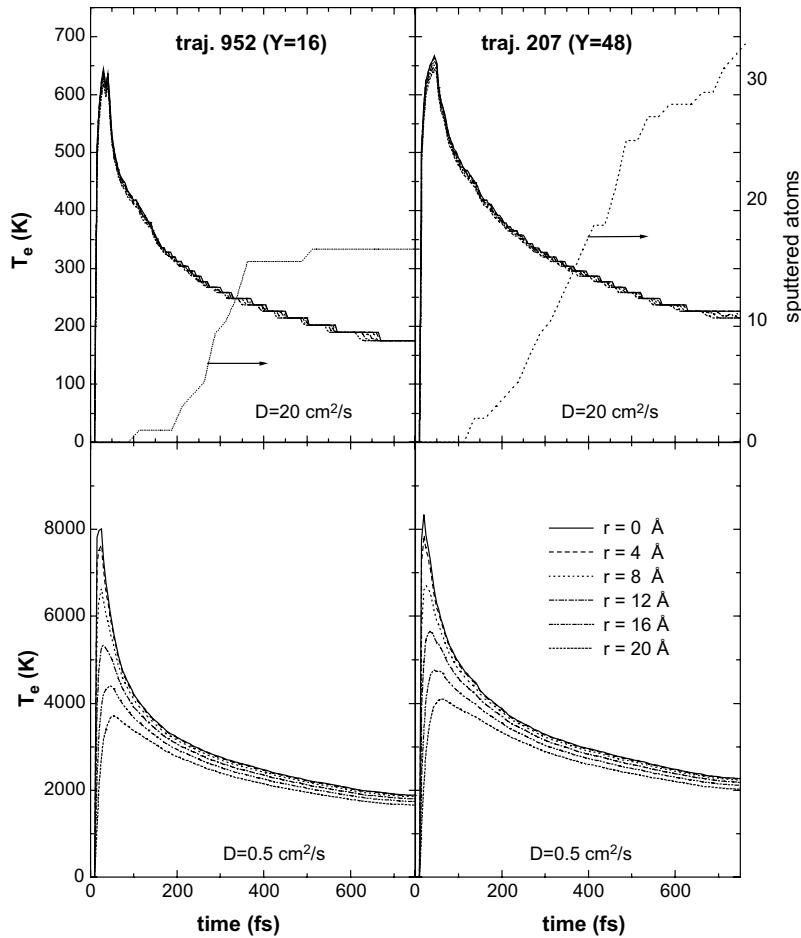


Fig. 6. Average surface electron temperature at different radial distances r from the impact point versus time after the projectile impact. The data were calculated for two different trajectories using a constant electron energy diffusion coefficient as displayed. The dotted line depicts the temporal evolution of sputtered particle emission.

completely amorphized crystal, respectively, and the results must therefore be regarded as limiting cases. It is seen that the projectile induced maximum T_e is most pronounced directly at the impact point. If heat diffusion is fast, the curves at larger radial distance completely track with that for $r=0$, thus indicating that the electron excitation is distributed homogeneously across the cascade volume. If diffusion is slow, on the other hand, it is clearly visible that the temperature rise at larger distance r is slower and the maximum is less pronounced than at $r=0$. At times exceeding approximately 500 fs, all curves are found to

merge to a “steady state” surface temperature, the inverse of which is found to linearly increase with increasing D . Note that the results calculated for both trajectories are almost identical, thus indicating that the details of the particular collision cascade are not important. This finding is understandable due to the large number of collisions involved in such a cascade. The time dependence of T_e can be compared to the temporal evolution of particle emission which has been included in the figure for both trajectories. It is evident that the majority of sputtered particles leave the surface at times later than 100 fs, thus making the sharp peak

of T_e at times below 100 fs practically unimportant for the determination of their charge or excitation states.

As already stated in Section 3.1, the temperature evolution depicted in Fig. 6 is not realistic since the diffusion coefficient will probably vary as a function of time due to collision induced atomic disorder. In order to arrive at a more realistic description of the transport of electronic energy within a collision cascade, we therefore invoke a time dependent D that is assumed to vary linearly from the crystal

limit at $t = 0$ to the amorphous limit at $t = t_{\text{am}}$ and remains constant thereafter. The resulting time evolution of the surface electron temperature is depicted in Fig. 7 for two different values of the amorphization time t_{am} . It is seen that the decrease of D during the cascade evolution leads to an increase and a second maximum of the electron temperature, which roughly occurs at $1.5t_{\text{am}}$.

This finding is particularly interesting, since the electronic excitation at the surface is now largest during the time period where most of the sputtered

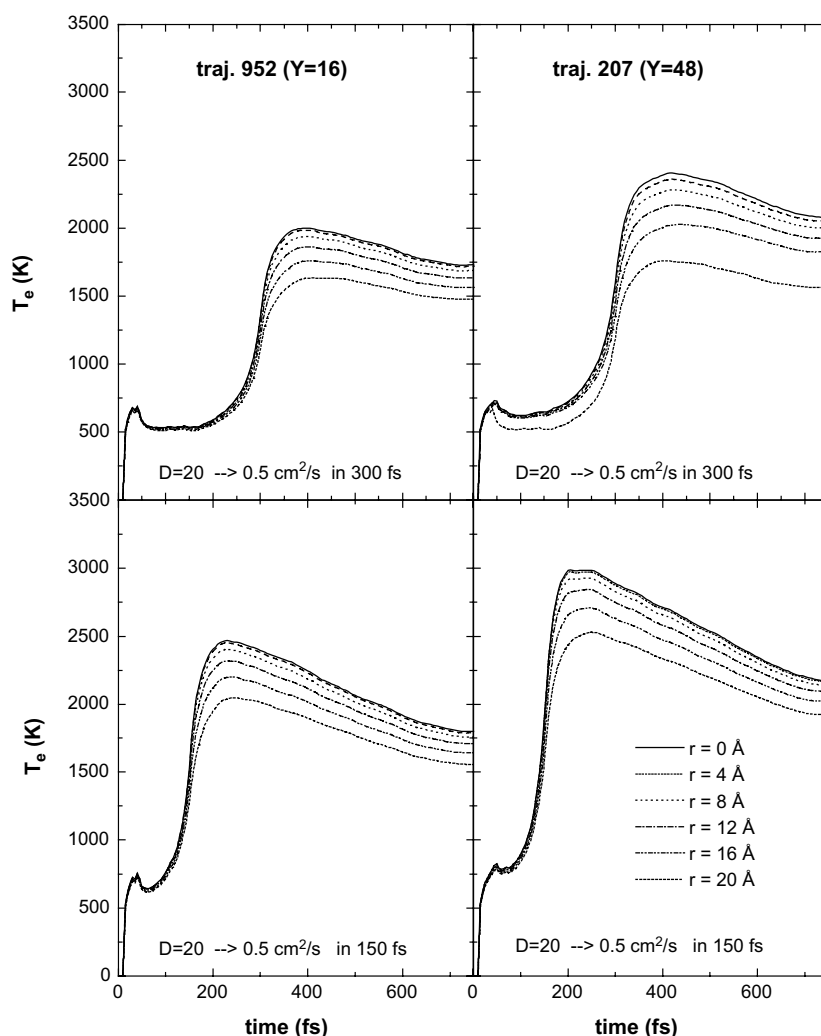


Fig. 7. Average surface electron temperature at different radial distances r from the impact point versus time after the projectile impact. The data were calculated for two different trajectories using a time dependent electron energy diffusion coefficient D as explained in the text.

particles are emitted (cf. Fig. 6). Moreover, the absolute values of the electron temperature are predicted to be of the order of 2000 K, a value which is sufficient to significantly influence the ionization and excitation probability of sputtered particles. More quantitatively, a simple estimate of the ionization probability using the ionization energy of Ag atoms (7.6 eV), the work function of silver (4.5 eV) and an image charge shift of about 1 eV in connection with an electron temperature of 2000 K yields values of the order of several 10^{-6} [37]. This is lower than the experimentally observed ionization probability of sputtered Ag atoms which has been measured to be of the order of 10^{-4} [38]. The apparent discrepancy may have several reasons. First, it is conceivable that the confinement and thus the concentration of electron–hole pairs in the dynamic collision cascade – during which the solid is in a highly non-equilibrium state – is larger than predicted by the diffusion equation, thus leading to higher values of T_e . Also the highly localized 4d holes created in Ag during ion bombardment [14] may play a role in the localization of excitation in the cascade. Another possibility is that the source term in (6) is considered to represent a lower limit and may be larger in the low-energy ion region than predicted by the LSS formula due to increasing contributions from electron–phonon coupling.

Finally, it should be noted that figures similar to Fig. 4 have been published by Koponen and Hautala [15] who employed a two-temperature model to describe the thermalization of a high-energy collision cascade. There are, however, a few fundamental differences which should be discussed in more detail. First, the electronic system treated in [15] is *assumed* to start with a high electron temperature which then decreases with time. This assumption clearly neglects the details of the short-term processes heating the electron gas which we are aiming at in the present study. Second, the data in [15] indicate that T_e remains essentially constant in the time range studied here, whereas our simulations predict a strong variation depending on the particular choice of the diffusion coefficient D . These differences are in part due to the different impact energy ranges explored in both studies (~ 100 keV in [15] versus keV here), but also reflect

the fact that the model described in [15] has been designed to describe the long-term temporal evolution of a collision cascade rather than the details of kinetic excitation during the first few hundred fs after the projectile impact.

4. Conclusion

A computer simulation model of the electron excitation in collision cascades in solids bombarded keV atomic particles has been developed. The model uses molecular dynamics for the simulation of atomic movements which excite the electrons and uses an approximate semiclassical approach for the description of spatial and temporal developments of the excitations. In this approach the excitations are characterized by the energy density of electron–hole pairs. The energy in the conduction band rapidly diffuses in space and thermalizes, creating a local electronic temperature T_e in the sp band. It is shown that the calculated surface temperature T_e can reach values of several thousands of Kelvin, thus showing that the electronic excitation process discussed here can influence the formation of slow ions and excited atoms emitted from solids during sputtering.

It is clear that the model presented here represents only a first step towards a microscopic understanding of the electronic excitation processes occurring in a collision cascade. On our way towards a more quantitative description, further studies will utilize the full four-dimensional $T_e(\mathbf{r}, t)$ profile in order to calculate the excitation and ionization probabilities of individual sputtered atoms. Moreover, a more appropriate description of the lattice order dependent diffusion coefficient is certainly needed for further improvement.

Acknowledgements

The authors are greatly indebted to B.J. Garrison for providing the basis of the molecular dynamics simulation code. We also acknowledge financial support from the Deutsche Forschungsgemeinschaft in the frame of the Sonderforschungsbereich 616 entitled “Energy Dissipation at

Surfaces". In part, this work was also supported by NSF (Grant No. CHE-0091328).

References

- [1] P. Sigmund, in: R. Behrisch (Ed.), *Sputtering by Particle Bombardment I*, Springer, 1981, p. 9.
- [2] W. Eckstein, *Computer Simulation of Ion–Solid Interactions*, Springer, 1991.
- [3] D.E. Harrison Jr., *Crit. Rev. Sol. State Mat. Sci.* 14 (1988) S1.
- [4] B.J. Garrison, N. Winograd, D.E. Harrison Jr., *Phys. Rev. B* 18 (1978) 6000.
- [5] M.H. Shapiro, T.A. Tombrello, *Nucl. Instr. and Meth. B* 90 (1994) 473.
- [6] Z. Srubek, G. Falcone, D. Aiello, C. Attanasio, *Nucl. Instr. and Meth. B* 88 (1993) 365.
- [7] Z. Srubek, *Phys. Rev. B* 25 (1982) 6046.
- [8] D.N. Bernardo, B.J. Garrison, *J. Chem. Phys.* 97 (1992) 6910.
- [9] R. Bhatia, B.J. Garrison, *J. Chem. Phys.* 100 (1994) 8437.
- [10] D.N. Bernardo, R. Bhatia, B.J. Garrison, *Comp. Phys. Comm.* 80 (1994) 259.
- [11] M.H. Shapiro, J. Fine, *Nucl. Instr. and Meth. B* 44 (1989) 43.
- [12] M.H. Shapiro, T.A. Tombrello, J. Fine, *Nucl. Instr. and Meth. B* 74 (1993) 385.
- [13] I. Wojciechowski, B.J. Garrison, *Surf. Sci.* 527 (2003) 209.
- [14] Z. Srubek, F. Srubek, A. Wucher, J.A. Yarmoff, *Phys. Rev. B* 68 (2003) 115426-1.
- [15] I. Koponen, M. Hautala, *Nucl. Instr. and Meth. B* 90 (1994) 396.
- [16] I. Koponen, *Phys. Rev. B* 47 (1993) 14011.
- [17] A. Caro, M. Victoria, *Phys. Rev. A* 40 (1989) 2287.
- [18] C.P. Flynn, R.S. Averback, *Phys. Rev. B* 38 (1988) 7118.
- [19] M. Beuve, N. Stolterfoht, M. Toulemonde, C. Trautmann, H.M. Urbassek, *Phys. Rev. B* 68 (2003) 125423-1.
- [20] B. Rethfeld, A. Kaiser, M. Vicanek, G. Simon, *Phys. Rev. B* 65 (2002) 214303-1.
- [21] J. Lindhard, M. Scharff, *Phys. Rev.* 124 (1961) 128.
- [22] C. Schaefer, H.M. Urbassek, L. Zhigilei V, *Phys. Rev. B* 66 (2002) 115404-1.
- [23] M. Lindenblatt, R. Heinrich, A. Wucher, B.J. Garrison, *J. Chem. Phys.* 115 (2001) 8643.
- [24] C.L. Kelchner, D.M. Halstead, L.S. Perkins, N.M. Wallace, A.E. DePristo, *Surf. Sci.* 310 (1994) 425.
- [25] A. Wucher, B.J. Garrison, *J. Chem. Phys.* 105 (1996) 5999.
- [26] O. Almén, G. Bruce, *Nucl. Instr. and Meth.* 11 (1961) 279.
- [27] B.A. Trubnikov, Yu.N. Yavlinskii, *Zh. Eksp. Teor. Fiz+* 48 (1965) 253.
- [28] M. Lindenblatt, E. Pehlke, personal communication.
- [29] D. Klushin, V.M.Y. Gusev, S.A. Lysenko, I.F. Urazgildin, *Phys. Rev. B* 54 (1996) 7062.
- [30] Z.G. Wang, C. Dufour, E. Paumier, M. Toulemonde, *J. Phys. Condens. Mat.* 6 (1994) 6733.
- [31] M. Brandbyge, P. Hedegard, T.F. Heinz, J.A. Misewich, D.M. Newns, *Phys. Rev. B* 52 (1995) 6042.
- [32] W.S. Fann, R. Storz, H.W.K. Tom, *Phys. Rev. B* 46 (2003) 13592.
- [33] C. Kittel, *Introduction to Solid State Physics*, John Wiley & Sons, 1971, p. 249.
- [34] P.M. Morse, H. Feshbach, *Methods of Theoretical Physics*, McGraw-Hill, 1953, p. 857.
- [35] X.Y. Wang, D.M. Riffe, Y.S. Lee, M.C. Downer, *Phys. Rev. B* 50 (1994) 8016.
- [36] D.S. Ivanov, L. Zhigilei V, *Phys. Rev. B* 68 (2003) 064114-1.
- [37] Z. Srubek, *Spectrochim. Acta* 44B (1989) 317.
- [38] M. Wahl, A. Wucher, *Nucl. Instr. and Meth. B* 94 (1994) 36.